



APPM4057 Project
Simulating Quantum Behaviours using Crank-Nicholson & Finite
Difference

Daniel Christodoulou
1690083

Anthony Ngankeu
2110906

Jason-leigh Smith
2135732

Paballo Mokoena
2128512

Gideon Ilung
2241186

1 Introduction

At a sub-atomic level the behaviours of physical systems deviate from the standard behaviour predicted by Newtonian mechanics. In order to model quantum behaviour, we must make use of Schrodinger's equation (1). This quantum behaviour can be seen in experiments like Young's double slit experiment. In this report two models are explored, the particle in a box and Young's double slit experiment. First we solve the 1D static Schrodinger's equation that describes the behaviour of a particle confined to a box. We then create a visual simulation for Young's double slit experiment and the 2D time-dependant particle in a box. For time-dependant problems, the wave function ψ is initialised using the Gaussian wave packet equation (2). We will replicate figures 5, 9 and 13 from [1] which are related to the above-mentioned problems.

$$\frac{\hbar^2}{2m} \nabla^2 \psi(\vec{x}, t) + V(x, y, z, t) \psi(x, y, z, t) = i \frac{\partial \psi}{\partial t} \quad (1)$$

$$\psi(\vec{x}, t = 0) = \mu \exp\left(-\left[\frac{(\vec{x} - \vec{x}_0)^2}{2\sigma^2}\right]\right) \exp(i\vec{k} \cdot \vec{x}) \quad (2)$$

1.1 Particle in a Box

The particle in a box model describes the behaviour of a particle free to move within a box that has impenetrable barriers. In order to enforce the condition of impenetrable barriers at the boundaries of the space region, we require that $\psi = 0$ outside the box, and at the boundaries of the box.

1.2 Young's Double Slit Experiment

The double slit experiment was first conducted by British physicist Thomas Young in 1801. The experiment comprises of a primary light source, two slits and a screen/detector. The experiment indicated that there is a wave nature to light as it depicted the diffraction pattern of light waves when a light source is made to pass through two slits that are in phase relative to one another. The light from one of the slits diffracts and constructively and destructively interferes with the light diffracted by the other slit, resulting in an interference pattern composed of bright bands and dark bands where the bright bands correspond to constructive interference and the dark bands correspond to destructive interference. The implication of these results led to the wave-particle theory of light in which light has both the properties of a particle and a wave.

2 Methodology

In the following section we discuss in detail the numerical techniques used to construct the various simulations.

2.1 1D Time Independent Schrodinger Equation

In the following section the numerical techniques used to solve the 1D Time Independent Schrodinger Equation (TISE) are discussed.

2.1.1 Determining the Energy Eigen-values

The 1D time-independent Schrodinger equation describing a particle in a box for which the potential $V(x) = 0$ is given as

$$-\frac{\hbar^2}{2M} \frac{d^2 \psi}{dx^2} = E \psi(x) \quad (3)$$

with boundary conditions $\psi(a) = \psi(b) = 0$. It is possible to calculate the energy eigenvalues by using finite difference scheme. Thus, we will have

$$\frac{d^2\psi}{dx^2} \approx \frac{\psi(x_i + 1) - 2\psi(x_i) + \psi(x_i - 1)}{\Delta x^2}. \quad (4)$$

Substituting equation (4) into equation (3), we obtain

$$-\frac{h^2}{2M\Delta x^2}(\psi(x_i + 1) - 2\psi(x_i) + \psi(x_i - 1)) = E\psi(x_i). \quad (5)$$

Equation (5) can be rewritten in matrix form as

$$-\frac{h^2}{2M\Delta x^2} \begin{bmatrix} 1 & -2 & 1 & 0 & \cdots & 0 \\ 0 & 1 & -2 & 1 & \cdots & 0 \\ \vdots & \vdots & \vdots & \vdots & \ddots & \vdots \\ 0 & 0 & \cdots & -2 & 1 & 0 \\ 0 & 0 & \cdots & 1 & -2 & 1 \end{bmatrix} \begin{bmatrix} 0 \\ \psi(x_1) \\ \vdots \\ \psi(x_{N-1}) \\ 0 \end{bmatrix} = E \begin{bmatrix} 0 \\ \psi(x_1) \\ \vdots \\ \psi(x_{N-1}) \\ 0 \end{bmatrix}. \quad (6)$$

By treating (6) as an eigen-value problem, we are able to determine the energy levels of the particle in a box, as well as the function $\psi(x)$ which characterizes the behaviour of the particle.

2.1.2 Shooting Method

In order to solve the TISE, the Shooting Method was selected, as other popular techniques such as collocation and spectral methods fail to solve the problem due to the homogeneity of the problem and the imposed boundary conditions being zero. As mentioned, the differential equation modelling the behaviour of the particle in a box is given as

$$\frac{h^2}{2M} \frac{d^2\psi}{dx^2} + E\psi(x) = 0. \quad (7)$$

Choosing $k = -\frac{2ME}{h^2}$, we may express the above equation as

$$\frac{d^2\psi}{dx^2} = k\psi(x). \quad (8)$$

This can then be expressed as a system of equations

$$y_1 = \psi(x), \quad (9)$$

$$y_2 = \frac{d\psi(x)}{dx}, \quad (10)$$

$$\frac{dy_1}{dx} = y_2, \quad (11)$$

$$\frac{dy_2}{dx} = ky_1. \quad (12)$$

Discretizing the system, the following equations are obtained

$$\frac{y_1^{i+1} - y_1^i}{\Delta x} = y_2^i, \quad (13)$$

$$\frac{y_2^{i+1} - y_2^i}{\Delta x} = ky_1^i. \quad (14)$$

By rewriting the system of equations and including the boundary conditions, we obtain

$$y_1^{i+1} = y_1^i + \Delta x y_2^i, \quad (15)$$

$$y_2^{i+1} = y_2^i + k\Delta x y_1^i, \quad (16)$$

$$y_1^0 = 0; \quad y_1^N = 0, \quad (17)$$

$$y_2^0 = z. \quad (18)$$

The goal of the Shooting Method is to determine the value of z such that the boundary conditions are satisfied. The Bisection Method was used to find the optimal z . A corresponding numerical solution is then obtained for each energy eigen-value.

2.2 2-D Particle in a Box & Young's Double Slit Experiment

In the following section the numerical solution of the 2-D time-dependant Schrodinger's equation is discussed. A Crank Nicholson, finite difference method is used to obtain a solution for

$$i \frac{\partial \psi}{\partial t} = -\frac{\partial^2 \psi}{\partial x^2} - \frac{\partial^2 \psi}{\partial y^2} + V\psi. \quad (19)$$

By applying the Crank-Nicolson scheme to 19, we obtain

$$i \frac{\psi^{n+1} - \psi^n}{\Delta t} = -\frac{1}{2} \left[\frac{\partial^2 \psi^{n+1}}{\partial x^2} + \frac{\partial^2 \psi^n}{\partial x^2} + \frac{\partial^2 \psi^{n+1}}{\partial y^2} + \frac{\partial^2 \psi^n}{\partial y^2} \right] + \frac{1}{2} [V^{n+1} \psi^{n+1} + V^n \psi^n]. \quad (20)$$

Then, by applying central difference on the terms $\frac{\partial^2 \psi}{\partial x^2}$ and $\frac{\partial^2 \psi}{\partial y^2}$, we obtain

$$\begin{aligned} i \frac{\psi^{n+1} - \psi^n}{\Delta t} = & -\frac{1}{2\Delta x^2} [\psi_{i+1,j}^{n+1} - 2\psi_{i,j}^{n+1} + \psi_{i-1,j}^{n+1}] \\ & -\frac{1}{2\Delta x^2} [\psi_{i+1,j}^n - 2\psi_{i,j}^n + \psi_{i-1,j}^n] \\ & -\frac{1}{2\Delta y^2} [\psi_{i,j+1}^{n+1} - 2\psi_{i,j}^{n+1} + \psi_{i,j-1}^{n+1}] \\ & -\frac{1}{2\Delta y^2} [\psi_{i,j+1}^n - 2\psi_{i,j}^n + \psi_{i,j-1}^n] \\ & + \frac{1}{2} [V_{i,j}^{n+1} \psi_{i,j}^{n+1} + V_{i,j}^n \psi_{i,j}^n]. \end{aligned} \quad (21)$$

By multiplying 21 by $\frac{\Delta t}{i}$ and setting $p_x = -\frac{\Delta t}{2i\Delta x^2}$ and $p_y = -\frac{\Delta t}{2i\Delta y^2}$, we obtain

$$\begin{aligned} & -p_x [\psi_{i+1,j}^{n+1} + \psi_{i-1,j}^{n+1}] + \left[1 + 2p_x + 2p_y + i\frac{\Delta t}{2} V_{i,j}^{n+1} \right] \psi_{i,j}^{n+1} - p_y [\psi_{i,j+1}^{n+1} + \psi_{i,j-1}^{n+1}] \\ & = p_x [\psi_{i+1,j}^n + \psi_{i-1,j}^n] + \left[1 - 2p_x - 2p_y - i\frac{\Delta t}{2} V_{i,j}^n \right] \psi_{i,j}^n + p_y [\psi_{i,j+1}^n + \psi_{i,j-1}^n]. \end{aligned} \quad (22)$$

By introducing

$$a_{i,j} = 1 + 2p_x + 2p_y + i\frac{\Delta t}{2} V_{i,j}^{n+1}, \quad (23)$$

and

$$b_{i,j} = 1 - 2p_x - 2p_y - i\frac{\Delta t}{2} V_{i,j}^n, \quad (24)$$

equation 22 can be simplified to

$$\begin{aligned} & -p_x [\psi_{i+1,j}^{n+1} + \psi_{i-1,j}^{n+1}] + a_{i,j} \psi_{i,j}^{n+1} - p_y [\psi_{i,j+1}^{n+1} + \psi_{i,j-1}^{n+1}] \\ & = p_x [\psi_{i+1,j}^n + \psi_{i-1,j}^n] + b_{i,j} \psi_{i,j}^n + p_y [\psi_{i,j+1}^n + \psi_{i,j-1}^n] \end{aligned} \quad (25)$$

Rewriting the LHS of equation 25 in matrix form

$$\begin{bmatrix} a_{00} & -p_x & 0 & 0 & \cdots & 0 & -p_y & 0 & \cdots & 0 \\ -p_x & a_{11} & -p_x & 0 & \cdots & 0 & 0 & -p_y & \cdots & 0 \\ \vdots & \vdots & \vdots & \vdots & \ddots & \vdots & \vdots & \vdots & \ddots & \vdots \\ -p_y & 0 & \vdots & \vdots & \ddots & \vdots & \vdots & \vdots & \ddots & \vdots \\ \vdots & \vdots & \vdots & \vdots & \ddots & \vdots & \vdots & \vdots & \ddots & -p_x \\ 0 & 0 & \cdots & \cdots & \cdots & \cdots & \cdots & \cdots & -p_x & a_{N-1,N-1} \end{bmatrix} \begin{bmatrix} \psi_{0,0}^{n+1} \\ \psi_{1,0}^{n+1} \\ \vdots \\ \psi_{i,j}^{n+1} \\ \vdots \\ \psi_{N-1,N-1}^{n+1} \end{bmatrix}.$$

Similarly, rewriting the RHS of equation 25 in matrix form

$$\begin{bmatrix} b_{00} & p_x & 0 & 0 & \cdots & 0 & p_y & 0 & \cdots & 0 \\ p_x & b_{11} & p_x & 0 & \cdots & 0 & 0 & p_y & \cdots & 0 \\ \vdots & \vdots & \vdots & \vdots & \ddots & \vdots & \vdots & \vdots & \ddots & \vdots \\ p_y & 0 & \vdots & \vdots & \ddots & \vdots & \vdots & \vdots & \ddots & \vdots \\ \vdots & \vdots & \vdots & \vdots & \ddots & \vdots & \vdots & \vdots & \ddots & p_x \\ 0 & 0 & \cdots & \cdots & \cdots & \cdots & \cdots & \cdots & p_x & b_{N-1,N-1} \end{bmatrix} \begin{bmatrix} \psi_{0,0}^n \\ \psi_{1,0}^n \\ \vdots \\ \psi_{i,j}^n \\ \vdots \\ \psi_{N-1,N-1}^n \end{bmatrix},$$

which results in a system of the form

$$A\psi^{n+1} = B\psi^n. \quad (26)$$

Since ψ contains complex values, it may be required to split the equation above into a system of 2 equations, one corresponding to the real part, and the other corresponding to the imaginary part. However, this is not necessary in Python. For Young's double slit experiment, the only additional criteria is that ψ must equal zero at the boundaries of the container.

3 Results

In this section we will discuss the results obtained by implementing the above-mentioned numerical techniques. These results will be compared with what we expect from the literature [1] and account for any discrepancies between the two.

3.1 Particle Confined in a Box

Solving for the eigenvalues of equation (6), we obtained the eigenvectors corresponding to the first ten energy levels of the particle confined to a box. We can view these resulting eigenvectors in the left plot of figure 1. It must be noted that each of these eigenvectors have been shifted up vertically for visual presentation. The plot on the right-hand side of figure 1 displays the approximated eigenvalues as well as the exact eigenvalues.

3.2 Free Propagation of 2D Gaussian Wave Packet

By solving the system derived by implementing a Crank-Nicolson and central difference scheme, we were able to obtain a simulation of the behaviour of the Gaussian wave packet as it propagates across a defined domain and is reflected off a surface. In figure 2 we can see there is a significant difference between the plot we obtain versus the plot found in [1]. The most notable difference is the amplitude of this wave packet, in our case, our function was normalised and so falls below an amplitude of 1. Furthermore, we can see that our time steps are different to those used in [1]. In our case, we used the Crank-Nicolson finite difference approach whereas in [1], they used the fourth order Runge-Kutta method. In order to increase the accuracy of the simulation, Crank-Nicolson was chosen to be applied in time as it has a higher order accuracy with regards to solving parabolic PDEs. Although, despite the differences in the employed numerical techniques, we can see a gradual decay in amplitude of the wave as it propagates and disperses into the environment. In figure 3 we can see the behaviour of the propagating packet of light from a top-down view.

3.3 Young's Double Slit Experiment

The way in which Young's double slit experiment was simulated was to take the problem of propagating a 2D Gaussian wave packet and then add a barrier with two equally spaced slits. In figure 4, we can readily

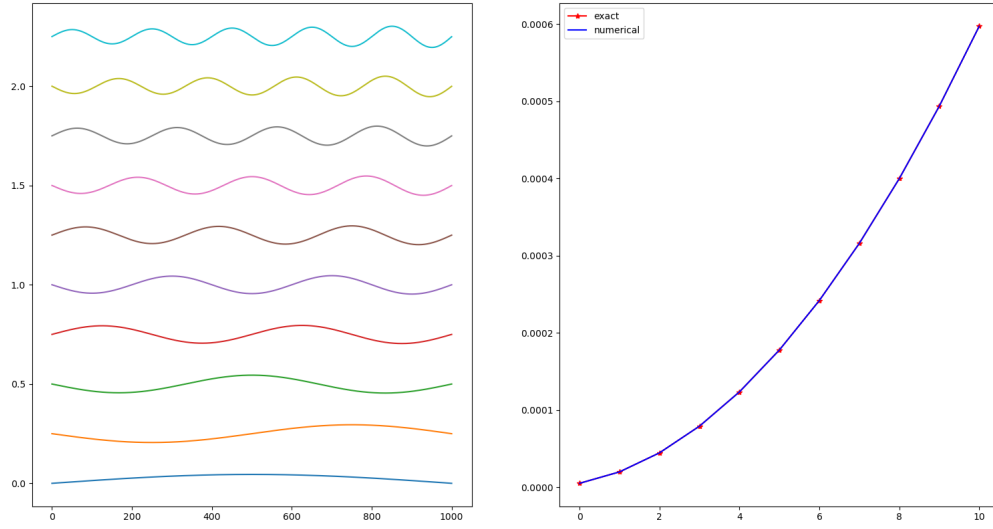


Figure 1: Left: Graphical plot of the eigenvectors corresponding to the first 10 eigenvalues for the time-independent Schrodinger's equation. Right: The first 10 eigenvalues calculated numerically as well as calculated analytically, given by $\frac{x^2 \pi^2}{2N^2 x}$

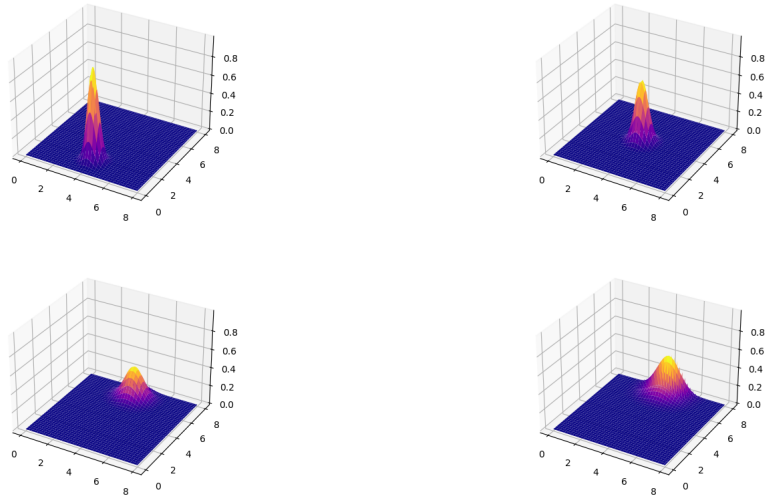


Figure 2: Free propagation and reflection of a 2D Gaussian wave packet, for times steps; $t=1$, $t=175$, $t=350$, and $t=500$.

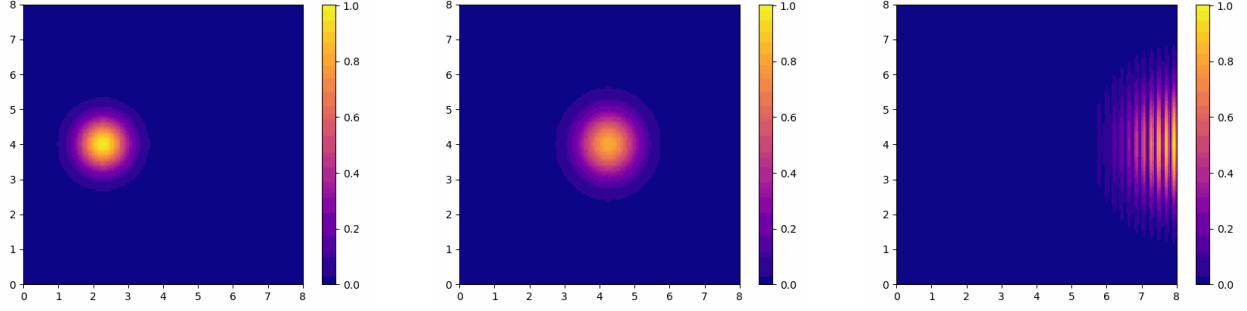


Figure 3: Behaviour of a Gaussian wave packet at different stages as it propagates and reflects.

observe the diffraction pattern caused by the interaction between the packet of light and the double slits, as well as the reflection of this packet of light when it encounters the barrier. If we now compare the set of images in figure 4 with those generated by [1], we can see that on the furthest plot to the left there is a difference between the initialised Gaussian packet of light. Our packet resembles a standard spherical Gaussian distribution, whereas, the Gaussian packet of light used in the [1] takes the shape of an ellipsoid. Additionally, there is certainly a difference in the sizing of the slits. Considering these difference, we can still recognise similarities between the two simulations. In the middle plot, we can see the same reflective pattern as the packet reflects off the barrier leading to bands of constructive and destructive interference. This pattern, however, changes in the right hand side plot, since we do not see the same four reflected bands of light seen in the corresponding figure in [1]. Additionally, we can consider the diffractive pattern of the light that passes through the slits. In this instance, the three bands of light is indeed reproduced, with additional light that surrounds these bands.

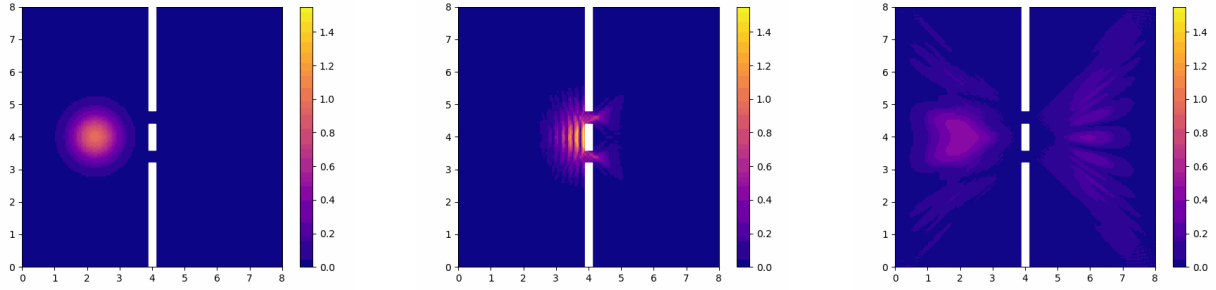


Figure 4: Behaviour of light particles at different stages in Young's double slit experiment.

4 Conclusion

From the results and figures gathered from the experiments we may conclude that Schrodinger's equation is a good abstraction of the system in question as the simulation results obtained closely mimic what is observed in reality. In this report numerical solutions to Schrodinger's equation are obtained in order to simulate quantum behaviours. The results were obtained using Python 3.8.10 running on Intel® Core™ i5-8400 CPU @ 2.80GHz \times 6, 16GB, 64-bit Ubuntu 22.04 LTS.

References

- [1] Etienne Thibierge Loren Jørgensen, David Lopes Cardozo. Numerical resolution of the schrödinger equation. Master's thesis, École Normale Supérieure de Lyon, 2011.